Journal of Applied Polymer Science

# Cyclodextrin-Dendrimer Functionalized Polysulfone Membrane for the Removal of Humic Acid in Water

**Soraya P. Malinga,[1] Omotayo A. Arotiba,[1] Rui W. M. Krause,[1] Selwyn F. Mapolie,[2] Mamadou S. Diallo,[1,3,4] Bhekie B. Mamba[1]**

[1]Department of Applied Chemistry, University of Johannesburg, Doornfontein 2028, South Africa

[2]Department of Chemistry and Polymer Science, University of Stellenbosch, Matieland 7602, South Africa

[3]Graduate School of Energy, Environment, Water and Sustainability (EEWS), Korea Advanced Institute of Science and Technology (KAIST), Daejeon 305-701, Republic of Korea

[4]Division of Engineering and Applied Science, Environmental Science and Engineering, California Institute of Technology, Pasadena, California 91125

Correspondence to: O. A. Arotiba (E-mail: oarotiba@uj.ac.za)

**ABSTRACT:** Commercial polysulfone (PSf) membranes were crosslinked with a β-cyclodextrin-poly (propyleneimine) (β-CD-PPI) conjugate which had β-CD pendant arms using trimesoyl chloride (TMC) by interfacial polymerization. The morphology and physicochemical properties of the nanofiltration membranes were characterized using Fourier transform infrared/attenuated total reflectance (FT-IR/ATR) spectroscopy, scanning electron microscopy (SEM), atomic force microscopy (AFM), and cross-flow filtration system. Water-contact angle, water-intake capacity, and rejection capacities of the membranes were evaluated. The β-CD-G4 (generation 4)-PPI-PSf and β-CD-G3 (generation 3)-PPI-PSf membranes both exhibited high humic acid rejection of 72% as compared to the commercial PSf which exhibited 57%. The modified membranes were also more hydrophilic (36° to 41°) than PSf (76°). These results suggest that β-CD-PPI nanostructures are promising materials for the synthesis of membranes for the removal of humic acid from water. © 2013 Wiley Periodicals, Inc. J. Appl. Polym. Sci. 000: 000–000, 2013

**KEYWORDS:** dendrimers; hyperbranched polymers and macrocycles; membranes; nanostructured polymers

Received 31 March 2013; accepted 2 July 2013; Published online 00 Month 2013

**DOI: 10.1002/app.39728**

## INTRODUCTION

Natural organic matter (NOM) is known to react with chlorine to produce disinfection by-products (DBPs) such as trihalomethanes which are generally toxic and exhibit mutagenic and carcinogenic properties.[1,2] Thus the removal of NOM from water systems is important due to the stringent regulations regarding DBPs and their impact on human health. NOM is made up of humic acid and fulvic acid. Humic acid, a principal component of humic substances, consists of high molecular weight long-chain molecules which are soluble in alkaline solution.[3] On the other hand, fulvic acid consists of low molecular weight molecules which are soluble in all pH ranges.[3] Because humic acid is the major component of NOM it is generally used as a model compound for NOM studies.[1]

The application of membranes for water treatment is of great research interest owing to their wide applicability and success rates.[4] The use of membrane technology in the water-treatment industry has become significant, and its demand increases yearly by 8%.[4] The quest for better membrane performance has necessitated the development of numerous membrane composites which are usually accomplished by the modification of a parent membrane material with other materials of interesting properties.[5,6] In this study, the polysulfone membrane was functionalized with poly (propyleneimine) dendrimer (PPI) and β-cyclodextrin (β-CD) as absorbents for the removal of humic acid from water. These two modifiers contain nanocavities which can encapsulate organics thus removing them from water.[7]

Poly(propylene imine) dendrimers (Figure 1) are macromolecules with highly branched three-dimensional structures. They consist of a diaminobutane core, interior branching units (propyleneimine), and peripheral (surface) $NH_2$ functional groups.[8] The interior branching units are usually called generations based on the number of repeated branches.[8] For example, if the interior consists of three and four repeated branches, the dendrimer

Additional Supporting Information may be found in the online version of this article.

© 2013 Wiley Periodicals, Inc.

Applied Polymer SCIENCE

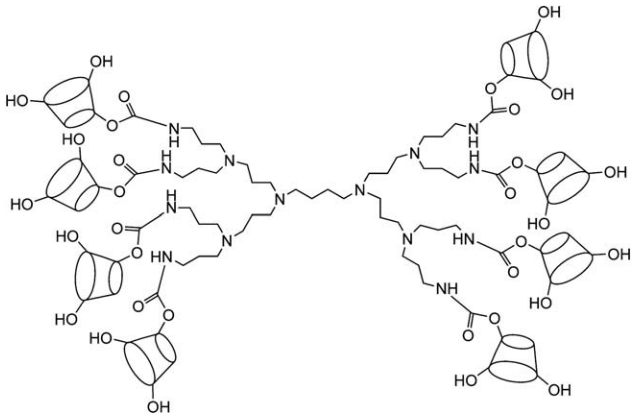

**Figure 1.** $\beta$-CD-PPI conjugate.

is called generation 3 (G3) and generation 4 (G4), respectively. In this study, generation 3 and generation 4 PPI dendrimers were used with 8 and 16 peripheral amine functional groups, respectively. The second modifier, $\beta$-CD, is a non-toxic stable cyclic oligosaccharide that has a hydrophobic cavity which can form inclusion complexes with a variety of solids, liquids and gaseous compounds. $\beta$-CDs have been polymerized using hexamethylene diisocyanate and toluene diisocyanate to form polymers which have been successfully used in the removal of organic pollutants from water.[9–11]

The application of $\beta$-CD polymer in the removal of humic acid from water has been reported by Mamba et al.[12] In this article, it was reported that the application of the $\beta$-CD resulted in a low removal efficiency of 23% when used in the treatment of humic acid.[12] This was attributed to the large size of the humic acid molecule (1.7–3.5 nm) as compared to the cyclodextrin cavity (0.62 nm) and hence the humic acid could not be accommodated as a guest within the cyclodextrin moiety.[12,13] In addressing this drawback, $\beta$-CDs were attached on the periphery of the poly (propyleneimine) dendrimers to form a conjugate system. Similar systems have been synthesized before and used in the medical field for drug- and gene-delivery applications.[14,15] However, to the best of our knowledge, the functionalization of $\beta$-cyclodextrin-poly (propyleneimine) ($\beta$-CD-PPI) conjugate onto a membrane for the removal of organic pollutants (such as humic acid) from water has not been reported.

On the application of either dendrimer or $\beta$-CDs (but not both) in membrane fabrication, Sarkar et al.[16] reported results obtained on a crosslinking reaction between a polyamidoamine dendrimer and polyethylene glycol which was prepared by a simple solution casting technique and used to modify a reverse-osmosis membrane. The resulting reverse-osmosis membranes had lower contact angles (19° to 21°), higher percentage salt rejection ($\approx$ 99%) and reduced flux (0.009 mL $cm^{-2}$ $min^{-1}$) as compared to the uncoated membranes.[16] In another study, the gas properties of polyimide membranes impregnated with various generations of poly (propylene imine)−6FDA-durene copolymers were investigated.[17] Generation 1 (G1) poly (propylene imine) 6FDA-durene membrane was found to have the highest gas permeability as compared to generation 2 (G2) and generation 3 (G3) membranes. This is because different dendrimers have different molecular sizes and reactivities.[17] Polyamidoamine dendrimer was crosslinked with polyethylene glycol and these materials were embedded on membranes and used to enhance the separation performance of carbon dioxide.[18] The polymeric membrane containing 50 wt % of the polyamidoamine dendrimer exhibited excellent ability to separate $CO_2$/$H_2$.[18] Commercial sized modules made from polyamidoamine dendrimers have also been developed and found to have a high $CO_2/N_2$ selectivity and $CO_2$ removal.[19] Moreover, PAMAM was incorporated onto crosslinked polyvinyl alcohol (PVA) membranes to produce a $CO_2$ selective membrane.[20] The PAMAM/crosslinked PVA membranes were found to be durable at high pressure and had improved $CO_2$ separation properties.[20] Hydrophilic and highly permeable $\beta$-CD polyurethane/PSf membranes have also been prepared using a modified phase-inversion method.[5] The resulting membrane resulted in cadmium rejection of up to 70%.[5] Recently, Choi et al.[21] prepared a hollow-fiber membrane with amphiphilic $\beta$-CD for the removal of di-(2-ethylhexyl) phthalate which is an endocrine-disrupting compound. The pure water flux and di-(2-ethylhexyl) phthalate removal efficiency (ca. 70%) increased considerably with the amount of $\beta$-CD loaded.[21] Furthermore, amine terminated $\beta$-CDs have also been incorporated into the polyamide membrane. The presence of $\beta$-CD cavities (0.62 nm) was found to provide capillary channels which were large enough for water (0.2 nm) to pass through as well as reject pollutants by size exclusion.[6] This improved the membrane flux and rejection of NaCl (86%) and $Na_2SO_4$ (94.7%) was achieved.

Various methods such as surface adsorption, coating, hydrophilization treatment, radical grafting, chemical coupling, plasma polymerization, initiated chemical vapor, and interfacial polymerization have been used in the surface modification of commercially available membranes.[22] Recently a novel polyester nanofiltration membrane was synthesized by the interfacial polymerization of triethonolamine and trimethyl chloride on a polysulfone supporting membrane.[23] This membrane was used in the rejection of different salt solutions such as $Na_2SO_4$ (82.2%), $MgSO_4$ (76.5%), NaCl (42.2%), and $MgCl_2$ (23%).[23] Kim and Deng[24] also fabricated a thin-film polyamide membrane with hydrophilized mesoporous carbon and this membrane was used in the adsorption of bovine serum albumin and salt rejection. With increasing amounts of mesoporous carbon (up to 6%), NaCl rejection was reduced from 68 to 50% and $Na_2SO_4$ from 94 to 90%.[24] Enantio-selective composite membranes were synthesized via interfacial polymerization with L-arginine, piperazine and trimesoyl chloride. These composite membranes have been successfully used in the separation of D-arginine and they are of great importance in the separation of numerous chiral drugs in the pharmaceutical industry.[25] In this study interfacial polymerization was used to form a thin-film composite on the surface of a commercial PSf membrane.

The above reports point to the beneficial effects of incorporating dendrimers and cyclodextrins in a membrane. This work reports the incorporation of $\beta$-CD-PPI into a commercial PSf ultrafiltration membrane to produce a novel composite membrane for the removal of humic acid in water.The composite membrane was extensively characterized while the pure water

**Table I.** Properties of Commercial PSf Ultrafiltration Membrane

| Properties | Commercial ultrafiltration PSf membrane |
|---|---|
| Pore size | 4.8 nm |
| Molecular weight cutt off | 10 kDa |
| Non woven support | polyester |
| Contact angle | 76° (hydrophobic) |

flux, water contact angle and water content of the membranes were measured.

## EXPERIMENTAL

### Materials

$\beta$-CD, from Wacker Chemie AG was donated by Industrial Urethanes. Generation 3 (G3) and generation 4 (G4) poly (propylene imine) dendrimers were purchased from SyMO-Chem B.V (Netherlands). *N,N*-carbonyldiimidazole(CDI) and 1,3,5-benzenetricarbonyl trichloride (TMC) were purchased from Sigma–Aldrich (USA). The humic acid was supplied by Fluka. The purification of the $\beta$-CD dendrimer conjugates was carried out using benzoylated dialysis tubing (Sigma–Aldrich, USA) with a molecular weight cut-off of 1200 g $mol^{-1}$. A commercial ultrafiltration PSf membrane (see properties in Table I) was supplied by Marsi Water (Northriding, South Africa).

### Synthesis of Precursor $\beta$-CD-CIm and $\beta$-CD-PPI

The precursor $\beta$-cyclodextrin carbonyl imidazole ($\beta$-CD-CIm) was first synthesized using a procedure reported in the literature with a few modifications (Scheme 1).[26] $\beta$-CD (0.845 g, 0.74 mmol) and carbonyldiimidazole (0.119 g, 0.77 mmol) were dissolved in dimethyl sulfoxide (6 mL) and stirred at room temperature for 1 h. Thereafter the solution was placed in an ice bath where diethyl ether (20 mL) was added to obtain a white precipitate. The white precipitate was filtered and washed several times with acetone. The product was dried under vacuum for 24 h at room temperature and a white powder (0.646 g, 69% yield) was obtained. The product was found to be soluble in both DMSO and water but insoluble in chloroform. FT-IR/ATR spectra showed the following peaks: 3286 $cm^{-1}$ (O—H), 2929 $cm^{-1}$ (C—C), 1697 $cm^{-1}$ (C═O), 1013 $cm^{-1}$, (C—O), 1382 $cm^{-1}$ (C—N), and 1635 $cm^{-1}$ (C═C). $^1$HNMR (400 MHz, DMSO-$d_6$) showed peaks at: $\delta$ (ppm) = 3.28–3.36 (m,-CH, cyclodextrin), $\delta$ (ppm) = 3.53–3.62 (m, -CH, cyclodextrin), $\delta$ (ppm) = 3.98 (b, OH, cyclodextrin), $\delta$ (ppm) = 4.82 (d, —CH, cyclodextrin, J = 4.00 Hz), $\delta$ (ppm) = 7.93 (s, imidazole), and $\delta$ (ppm) = 7.67 (d, imidazole, J = 1.08 Hz). $^{13}$C NMR (400 MHz, DMSO-$d_6$,) showed peaks at: $\delta$ (ppm) = 162.5 (NHC═O, imidazole), $\delta$ (ppm) = 134.3 (CH═CH—N═CH, imidazole), $\delta$ (ppm) = 119.4 (CH═CH—N═CH, imidazole), $\delta$ (ppm) = 102 (O—C—O, cyclodextrin), $\delta$ (ppm) = 81.6 (C—O, cyclodextrin), $\delta$ (ppm) = 72.1 (C—OH, cyclodextrin), $\delta$ (ppm) = 73.1 (C—OH, cyclodextrin), $\delta$ (ppm) = 60.0 (—$CH_2$OH), $\delta$ (ppm) = 30.98 (—$CH_2$—), and $\delta$ (ppm) = 36.7 (N—CH, imidazole).

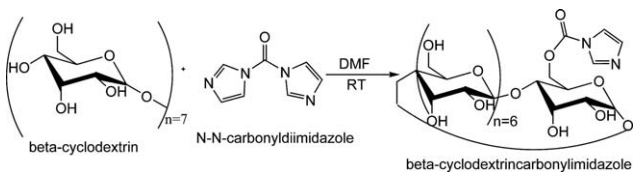


**Scheme 1.** Synthetic route for the preparation of $\beta$-CD-CIm.

A typical conjugation reaction of the $\beta$-CD-CIm precursor and poly (propyleneimine) dendrimer (generation 3 and generation 4) as depicted in Scheme 2, was carried out as follows: Generation 3 poly (propylene imine) (G3-PPI) (0.211 g, 0.125 mmol) was dissolved in dimethyl sulfoxide (3 mL); the $\beta$-CD-CIm (2.446 g, 1.9 mmol) and triethylamine (3 mL) were added to this dendrimer solution.[26] This solution was stirred at room temperature for 24 h and purified using dialysis against deionized water for 2 days. Lyophilization of the solution for 2 days resulted in a white fluffy solid (776 mg, 31.3%). FT-IR/ATR spectra showed the following peaks: 3286 $cm^{-1}$ (O—H), 2929 $cm^{-1}$ (C—C), and 1 697 $cm^{-1}$ (NH—C═O). $^1$HNMR (400 MHz, DMSO-$d_6$,) showed peaks at: $\delta$ (ppm) = 1.62 (—$CH_2$, dendrimer), $\delta$ (ppm) = 2.81 ($CH_2$NH, dendrimer), $\delta$ (ppm) = 2.65 ($CH_2$N, dendrimer), $\delta$ (ppm) = 3.49–3.59 (m, —CH, cyclodextrin,), $\delta$ (ppm) = 3.77–3.88 (m, —CH, cyclodextrin), $\delta$ (ppm) = 5.00 (s, —$CH_2$, cyclodextrin), and $\delta$ (ppm) = 7.60 (s, NH—C═O). $^{13}$C (DEPT, 135: 100 MHz) showed peaks at: $\delta$ (ppm) = 22.42, 23.85, 25.57, 35.67, 50.34 (—$CH_2$, dendrimer), $\delta$ (ppm) = 58.73 (—$CH_2$, cyclodextrin), and $\delta$ (ppm) = 70.86, 71.23, 71.88, 80.35, 100.77 (—CH, cyclodextrin).

Generation 4 poly (propyleneimine) (G4-PPI) (0.205 g, 0.058 mmol) was dissolved in dimethyl sulfoxide (3 mL). The $\beta$-CD-CIm (2.34 g, 1.81 mmol) and triethylamine (3 mL) were added to the dendrimer solution.[26] This mixture was stirred for 24 h at room temperature and the product was purified using dialysis against deionized water for 2 days. Lyophilization of the solution for 2 days resulted in a white fluffy solid (550 mg, 23.8%). FT-IR/ATR spectra showed the following peaks: 3286 $cm^{-1}$(O—H), 2929 $cm^{-1}$ (C—C), and 1697 $cm^{-1}$ (NH—C═O). $^1$HNMR (400 MHz, DMSO-$d_6$,) showed peaks at: $\delta$ (ppm) = 1.57–1.62 (—$CH_2$, dendrimer), $\delta$ (ppm) = 2.33 ($CH_2$N, dendrimer), $\delta$ (ppm) = 2.6 ($CH_2$NH, dendrimer), $\delta$ (ppm) = 3.28–3.34 (m, —CH, cyclodextrin), $\delta$ (ppm) = 3.54–3.61 (m, —CH, cyclodextrin), $\delta$ (ppm) = 4.82 (s, —CH, cyclodextrin), and $\delta$ (ppm) = 7.94 (s, NH—C═O).$^{13}$C (DEPT, 135: 100 MHz) showed peaks at: $\delta$ (ppm) = 23.94, 26.72, 38.30, 51.43 (—$CH_2$, dendrimer), $\delta$ (ppm) = 59.86 (—$CH_2$, cyclodextrin), and $\delta$ (ppm) = 71.99, 72.36, 73.01, 81.48, 101.90 (—CH, cyclodextrin).

### Preparation of $\beta$-CD-PPI-PSf Membrane

The membranes were prepared by using an interfacial polymerization reaction. An aqueous phase solution was prepared by dissolving the G3 or G4 $\beta$-CD-PPI dendrimer conjugate (6%, w/v) in water. The microporous commercial PSf membrane was then coated with the aqueous solution for 24 h at room temperature. The membrane was then immersed in the organic phase solution, i.e. trimesoyl chloride (1% w/v) in n-hexane for 60 s. The membrane was thereafter dried in an oven at a temperature of 60°C for a period of 30 min to promote further

Applied Polymer SCIENCE

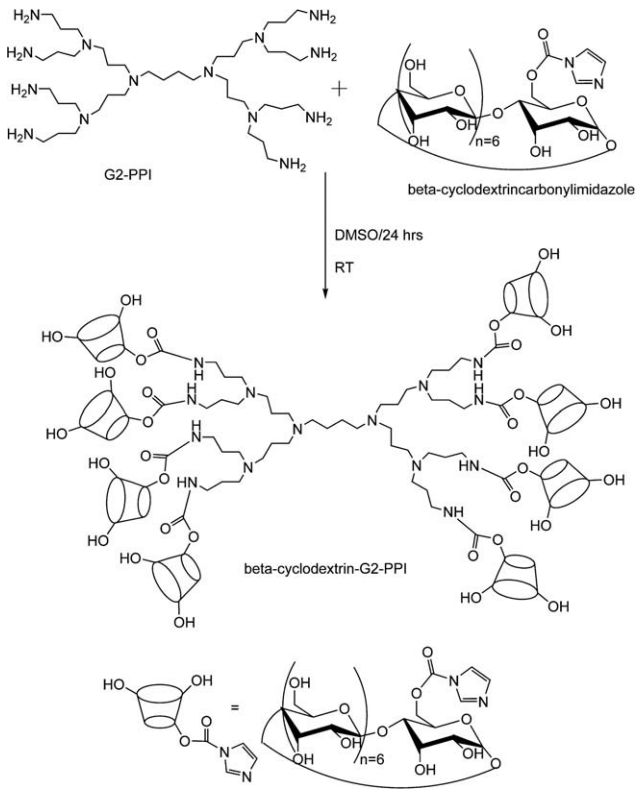


**Scheme 2.** Typical synthetic route for the preparation of *β-G2*-CD-PPI conjugate (G3: 16 —$NH_2$: 16 CD molecules, G4: 32 —$NH_2$: 32 CD molecules).

polymerization. The modified PSf membranes were then washed with deionized water to remove any of the residual trimesoyl chloride and stored in deionized water until further use.

### Instrumentation

**Nuclear Magnetic Resonance (NMR).** The $^{1}H$-, $^{13}C$-, NMR analyses were carried out using a Bruker 400 MHz NMR spectrophotometer. All chemical shifts ($\delta$) are expressed in ppm relative to residual solvent peak or TMS. The following terms are used to explain multiplicities: s = singlet, d = doublet, m = multiplet.

**Fourier Transform Infrared/Attenuated Total Reflectance (FT-IR/ATR) Spectroscopy.** *β*-CD-CIm, *β*-CD-PPI and the membrane samples were analyzed with a Perkin Elmer 100 FT-IR spectrophotometer. Powder and membrane samples (with coated layer facing down) were placed on the ATR and analyzed in the range of 650–4000 $cm^{-1}$ averaging 32 scans and at a spectral resolution of 4 $cm^{-1}$.

**Thermogravimetric Analysis (TGA).** The thermal properties and stability of poly (propyleneimine), *β*-CD-CIm and *β*-CD-PPI were assessed using a Perkin Elmer TGA (400) with a heating rate of 10°C $min^{-1}$ over a temperature range of 25–800°C under a nitrogen atmosphere.

**Microscopy (Scanning Electron Microscopy-Energy Dispersive X-ray Diffraction Spectroscopy and Atomic Force Microscopy).** Field emission scanning electron microscopy (Joel, JSM, 7500F) coupled with energy dispersive X-ray diffraction (EDX) was used to determine the morphologies of the PSf and the modified membranes. The samples were coated with gold twice at 20 mA for 2 min.

A multimode atomic force microscope (AFM) nano-scope version (IV) was used to determine surface morphology and roughness ($R_q$) of the membranes. The membrane sample (1 cm × 1 cm) was placed on a sample holder and the RTESPW tip with a radius of curvature of <10 nm (Veeco Instruments) was used. The tip was mounted on a 125-$\mu$m-long cantilever beam with a spring constant of 40 N $m^{-1}$ and this was employed for the tapping-mode experiment. The height and phase images were obtained using a scan rate of 0.5 Hz and the tip frequencies ranged from 280 to 310 kHz.

**Contact-Angle Analysis.** Contact-angle analyses were measured using the sessile-drop method on a Data Physics OCA (Optical Contact Angle) instrument. About 5–10 measurements were conducted at different sites per sample and all measurements were recorded at room temperature. These analyses were carried out in order to determine the hydrophilicity of the membranes.

**Grafting Yield.** The grafting yields of the membranes were calculated as the mass increase of the membrane after the grafting, which is given in eq. (1)[27]:

$$G(\%) = \frac{m_c - m_o}{m_o} \times 100 \quad (1)$$

where $G$ is the mass gain, $m_o$ is the mass of the membrane prior to grafting, and $m_c$ is the mass of the grafted and dried membrane.

### Water-Intake Capacity and Porosity Measurements

Water-intake capacity was performed to evaluate the adsorption of water by the fabricated membranes. The water-intake capacity of the membrane was obtained after soaking the membrane in deionized water for 24 h. The membranes were weighed after mopping with paper to obtain the wet weight. The membranes were dried in an oven at 60°C for 24 h to obtain the dry weight. The per cent water-intake capacity (WIC) was calculated using eq. (2)[5]:

$$\mathrm{WIC}\,(\%) = \frac{W_w - W_d}{W_w} \times 100 \quad (2)$$

where $W_w$ and $W_d$ are the wet and dry weights of the membrane, respectively.

Membrane porosity was determined by immersing the membrane in water for 24 h followed by blotting the membrane with paper and thereafter weighing the membrane to obtain its wet weight. The membrane was then dried in an oven at 60°C for 24 h and the dry weight was obtained. The porosity of the membrane ($P$) was measured by using eq. (3):

$$P\ (\%) = \frac{(W_o - W_1)}{Ah} \times 1000 \quad (3)$$

where $W_o$ and $W_1$ are the weights of the wet and dry membrane, respectively, $A$ is the area of the membrane ($cm^2$), and $h$ is the membrane thickness (mm).

### Separation Performance Tests

The separation performance tests of *β*-CD-PPI membranes and PSf were evaluated using a six-cell cross-flow parallel membrane

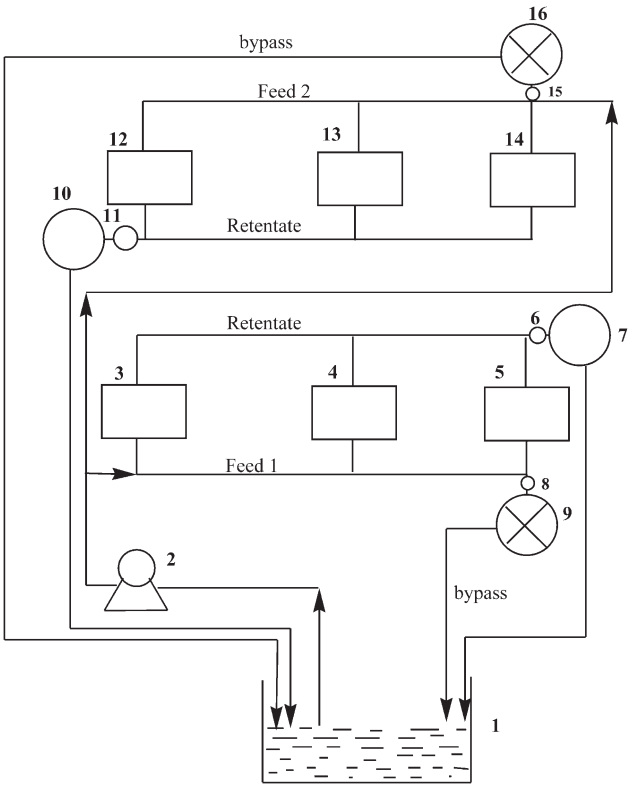


**Scheme 3.** A schematic representation of a six cell crossflow system. (1) Feed solution (10 L, 22°C); (2) Feed pump; (3–5) and (12–14) Membrane cell; (6 and 11) Back pressure regulators; (7 and 10) Flow meter; (8 and 15); By pass valves; (9 and 16) Pressure gauges.

system shown in Scheme 3. The membranes were stabilized at 20 bar for 2 h with deionized water before testing. The six-cell cross-flow system has a set of membrane cells fed in parallel from a single feed tank.[28] The water in the feed tank was maintained by magnetic stirring and was pumped out of the reservoir and pressurized in the system by a hydra-cell pump. A laboratory recirculating heater chiller (Poly Science Digital Temperature Controller) maintained the feed-water temperature at 22°C. The back pressure regulators (Swagelok) and bypass valves controlled the feed-water hydraulic pressure and cross-flow velocity for each side individually.[28] After sampling, the permeate and retentate were returned back to the feed tank in order to maintain a constant concentration of the humic acid.

The membrane permeability was determined from pure water flux using deionized water. The water flux ($J_v$) is expressed as in eq. (4)[5]:

$$J_v = \frac{V}{At} \tag{4}$$

where $v$ is the permeate volume ($\ell$), $A$ is the effective membrane area (0.00129 $m^2$), and $t$ is the time (h) to collect the permeate volume.

To evaluate the performance of the membrane in terms of humic acid rejection efficiency, the feed solution of humic acid (50 mg $L^{-1}$) was passed through the membrane at a constant pressure of 6.89 bar. The flux was monitored every 20 min for over an hour and the permeate was only collected once after 40 min. The permeate was analyzed using a UV–vis spectrophotometer at 254 nm. The percentage rejection (%R) of humic acid was calculated using eq. (5).

$$\%R = 1 - \frac{c_p}{c_f} \times 100 \tag{5}$$

where $C_p$ is the concentration of the permeate and $C_f$ the concentration of the feed (mg $L^{-1}$).

### Membrane Pore Size Calculations

The pore sizes of the PSf support and $\beta$-CD PPI PSf membrane were estimated using the steric exclusion model.[29] This model estimates the pore size from the single solute rejections and the solute rejection is related to the solute-to-pore size ratio according to eq. (6):

$$X_s = [\lambda(2-\lambda)]^2 \tag{6}$$

where $\lambda = r_s/r_p$ is the solute-to-pore size ratio, $r_s$ is the radius of humic acid, and $r_p$ is the radius of the membrane pores.

The humic acid effective diameter was determined by using eq. (7)[30]:

$$r_E = 0.0625(\mathrm{MW})^{0.438} \tag{7}$$

where $r_E$ is the particle diameter (nm) and MW is the molecular weight of the humic acid.

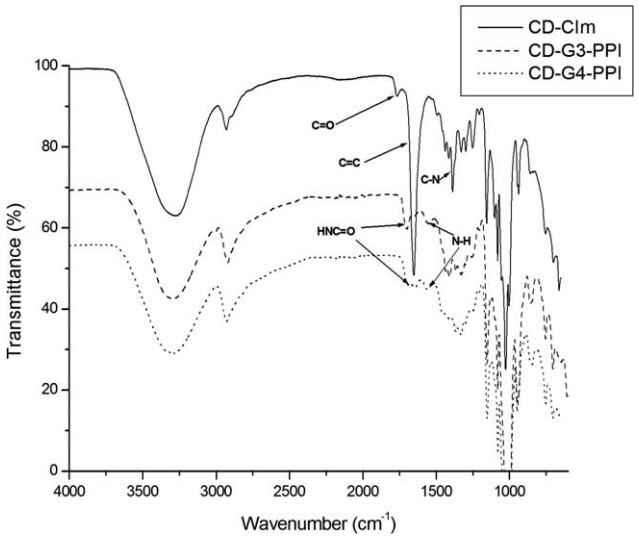


**Figure 2.** FTIR spectrum showing comparison between $\beta$-CDCIm, $\beta$-CD-G3-PPI and $\beta$-CD-G4-PPI conjugates.

## RESULTS AND DISCUSSION

### FT-IR/ATR and NMR Analyses

The FT-IR spectra of $\beta$-CD-CIm, $\beta$-CD-G3-PPI and $\beta$-CD-G4-PPI are shown in Figure 2. The incorporation of the imidazole into the $\beta$-CD backbone to form $\beta$-CD-CIm was confirmed by FT-IR spectroscopy. An intense band was detected at 1635 $cm^{-1}$ which is due to the C=C vibration from the imidazole ring.

Applied Polymer SCIENCE

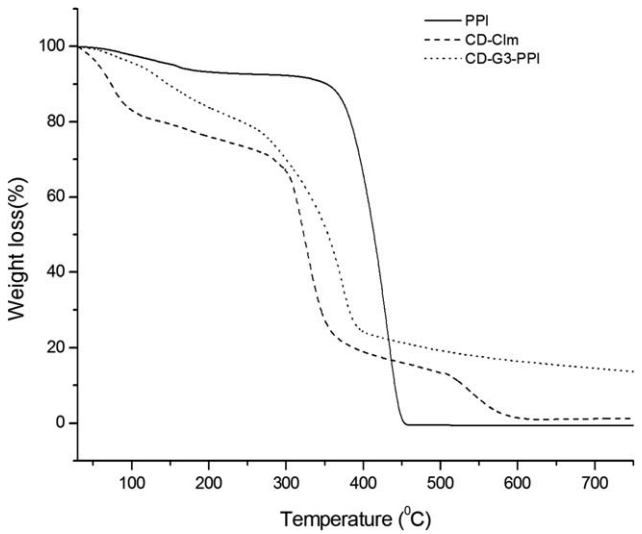


**Figure 3.** TGA analysis for: PPI, β-CD-CIm and β-CD-G3-PPI.

Moreover, the carbonyl peak at 1765 $cm^{-1}$ (C═O) gave further confirmation that the carbonyldiimidazole had been transferred to β-CD via substitution of some of the hydrogen atoms.

The β-CD dendrimer materials (β-CD-G3-PPI and β-CD-G4-PPI) show the appearance of a new peak at 1697 $cm^{-1}$ which is attributed to the amide peak of the newly formed amide bond.[26] The disappearance of the sharp band at 1635 $cm^{-1}$ gave further evidence that the imidazole ring had been displaced by the $NH_2$ groups of the dendrimer. In addition, the C═N peak at 1382 $cm^{-1}$, due to the imidazole ring, also disappeared after the reaction with the PPI dendrimer. A small broad peak at 1600 $cm^{-1}$ in the spectrum of the conjugate can be assigned to the N═H bend from the PPI dendrimer indicating that the β-CD-CIm was converted to the β-CD-G3-PPI and β-CD-G4-PPI conjugates.

The proton NMR spectrum of β-CD-CIm (Supporting Information Figure S1) gave the characteristic peaks of the imidazole group in the aromatic region. The peaks were identified as a singlet and a doublet at $\delta$ (ppm) = 7.93 and $\delta$ (ppm) = 7.67, respectively. The singlet peak appearing at $\delta$ (ppm) = 4.82 is due to the hydroxyl proton at position 6 of the β-CD integrated for 6 protons. This showed that the imidazole was successfully functionalized at position 6 of the β-CD (Scheme 1). The $^{13}$CNMR spectra (Supporting Information Figure S2) showed the appearance of new downfield peaks associated with the imidazole ring at $\delta$ (ppm) = 162.5, $\delta$ (ppm) = 134.3 and $\delta$ (ppm) = 119. The downfield shift is associated with the high de-shielding effect of the highly electronegative nitrogen atoms on the imidazole ring.

The $^{1}$HNMR studies also revealed that the poly (propylene imine) dendrimer was successfully conjugated to the β-CD (Supporting Information Figure S3). The dendrimer methylene protons resonated at $\delta$ (ppm) = 2.80, $\delta$ (ppm) = 2.65 and $\delta$ (ppm) = 1.61 and a very weak signal of the amide proton (HNC═O) was observed downfield as a singlet at $\delta$ (ppm) = 7.94 (Supporting Information Figure S3: insert). The cyclodextrin part of the molecule appears as a set of well-resolved signals in the region $\delta$ (ppm) = 3.59 to $\delta$ (ppm) = 4.99. These results are in agreement with those reported in the literature, where PPI was also conjugated with β-CD.[26] The $^{13}$C DEPT analysis of β-CD-G2-PPI conjugate in DMSO is shown in Supporting Information Figure S4. This spectrum shows well-resolved peaks that were assigned to the ─CH groups ($\delta$ (ppm) = 71, $\delta$ (ppm) = 80, $\delta$ (ppm) = 100) and a very sharp peak due to the ─$CH_2$ groups ($\delta$ = 58) associated with β-CD. The remaining carbon signals at $\delta$ (ppm) = 22, $\delta$ (ppm) = 23, $\delta$ (ppm) = 25, $\delta$ (ppm) = 36 and $\delta$ (ppm) = 56 were assigned to the methylene groups of the PPI dendrimer. These dendrimer chemical shifts conform to the $^{13}$CNMR analysis of PPI methylene groups at $\delta$ (ppm) = 26, $\delta$ (ppm) = 27, $\delta$ (ppm) = 32, $\delta$ (ppm) = 41, $\delta$ (ppm) = 52 and $\delta$ (ppm) = 56 reported in the literature.[31] These results suggest that the dendrimer and the β-CD had formed a conjugate.

### TGA Analysis of the PPI, β-CD-CIm, and β-CD-G3-PPI Conjugates

The thermogravimetric analyses (Figure 3) for the unmodified PPI dendrimer, β-CD-CIm and β-CD-G3-PPI were conducted at a heating rate of 10°C $min^{-1}$ in a nitrogen atmosphere (20 mL $min^{-1}$). The PPI, β-CD-CIm, and β-CD-G3-PPI each underwent water loss at ~100°C. The PPI dendrimer completely decomposed at 380°C (weight loss ~90%), while the other material decomposed at much lower temperatures. Comparison of the onset temperature of decomposition of the precursors PPI (380°C) and β-CD-CIm (300°C) to that of the conjugate β-CD-G3-PPI (290°C) revealed a slight decrease in decomposition temperature. The lower stability of the conjugates compared to that of the pure poly (propyleneimine) dendrimer has been reported.[7] Polyamidoamine-cyclodextrin copolymer was found to decompose at 235°C and this might be due to the addition of cyclodextrin resulting in amorphous material.[7] However, the decrease in stability of the β-CD-G3-PPI is not significant when considered in terms of the proposed water-treatment application. These observations reveal that the conjugates can be used for relatively high-temperature applications.

### Fabrication of β-CD PPI PSf Membrane

**Characterization of the Surface Layer of the Membrane.** To obtain information about structural modification of the PSf membrane after interfacial polymerization of β-CD-PPI conjugate and trimesoyl chloride, FT-IR analyses were performed. Interfacial polymerization is carried out by a poly-condensation reaction of a polyfunctional amine or polyol (aqueous phase) with an acid chloride (organic phase) at the interface of two immiscible solvents to produce a membrane with a crosslinked layer.[29,32] The results given in Figure 4 indicate that the polymerization had occurred since there is disappearance of the carbonyl bond of the acid chloride band at 1744 $cm^{-1}$ and three new bands at 3352, 1796, and 1708 $cm^{-1}$ which are characteristic of $\nu$(OH), $\nu$(O─C═O) and $\nu$(HN─C═O) vibrations were detected for the β-CD-PPI-PSf membrane. The absorption bands at 3352 and 1708 $cm^{-1}$ are due to hydroxyl groups and the amide bond from the β-CD-PPI monomer (see Figure 2) and this gave confirmation that the β-CD-PPI monomer was incorporated into the PSf membrane. The peak at 1796 $cm^{-1}$ is characteristic of an ester group suggesting that a polyester film

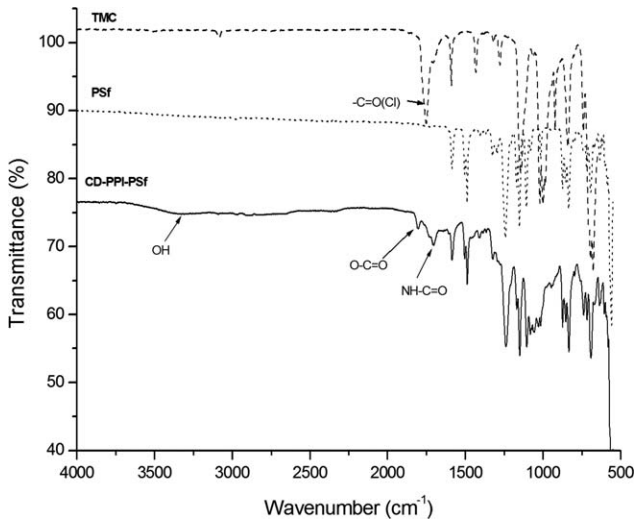


**Figure 4.** FTIR spectrum showing comparison between TMC, PSf membrane and β-CD-PPI-PSf membrane.

was formed and the possible mechanism of chemical bonding between β-CD-PPI dendrimer and trimesoyl chloride is illustrated in Scheme 4. The β-CD-PPI is attached via covalent bond or hydrogen bonding between the hydroxyl groups of the β-CD-PPI and the sulfonyl groups of the PSf.[5]

**SEM Analyses.** The changes in surface morphologies between the unmodified PSf membrane and the β-CD-PPI modified PSf membranes can be distinctly observed in Figure 5. The surface of the PSf membrane is smooth and featureless as shown in Figure 5(A). After interfacial polymerization on the surface of the PSf at 500× magnification, a rough surface layer was generated [Figure 5(B)]. At higher magnification [Figure 5(C)] the thin-film composite appears as a dense layer with an even distribution of circular white particles on the surface of the membranes. The presence of these particles has been observed before on the surface of a nanofiltration membrane developed from hydroxyl terminated hyperbranched polyester (HPE) and trimesoyl chloride during interfacial polymerization.[33] The formation of these particles on the surface of the membrane is due to the congregation and intramolecular reaction of the HPE molecules, resulting in HPE particles being present on the surface of the membrane.[33] These white circular particles observed on the SEM micrographs were from the β-CD-PPI monomer.

**AFM Studies.** AFM analyses were also carried out in 2D and 3D mode at 4 μm scan to further investigate any changes in surface morphology [Figure 6(A–F)]. The 3D AFM image revealed that the PSf surface was flat, evenly distributed and had a uniform ridge-and-valley structure illustrated in Figure 6(A,B). After interfacial polymerization of the β-CD-PPI monomer with trimesoyl chloride, the membrane topography showed new protrusions which were unevenly distributed for β-CD-G3-PPI-PSf [Figure 6(C,D)] and β-CD-G4-PPI-PSf [Figure 6(E,F)]. These AFM analyses are consistent with what has been reported in the literature where similar membrane modifications were performed.[5,33,34] Kang et al.[34] observed that the ridge-and-valley pattern of the unmodified membranes became irregular with an increase in roughness from 58 to 98 nm after polyethylene glycol modification. The roughness measurements of 6.34 nm for unreacted PSf in comparison to 9.55 and 23.55 nm for β-CD-CD-G3-PPI-PSf and β-CD-G4-PPI-PSf, respectively, were similar to findings reported by Kang et al.[34] In general, roughness was found to increase due to the various manufacturing process steps (i.e. from PSf to β-CD-PP-PSf).[33] As seen in the SEM micrographs, the AFM results again confirmed that the β-CD-PPI monomer was successfully grafted onto the surface of the membrane. Moreover, the grafting yield percentage shown in Table I also confirmed the attachment of the β-CD-PPI on the surface of the membrane.

**Membrane Separation Studies.** ***Permeation and rejection characteristics.*** The water-intake capacity, porosity, grafting yield, contact angle and pure water permeability are shown in Table II. The water-contact angles in this study are used as a direct indication of hydrophilicity of the membranes. It can be observed that the addition of the β-CD-PPI monomer enhanced the hydrophilicity of the membrane shown by a decrease in contact angle from 76° for unmodified PSf to 36 and 41° for β-CD-G3-PSf and β-CD-G4-PSf, respectively. The enhancement of the surface hydrophilicity of the modified PSf membranes was attributed to the introduction of hydrophilic —OH and —NH groups from the β-CD molecule and poly (propyleneimine) dendrimer, respectively. During the interfacial polymerization, partial reaction of the —OH groups was effected by reducing the trimesoyl chloride concentration used as well as the time taken for the crosslinking reaction. The presence of unreacted —OH groups was noted in the FT-IR spectra of the modified membrane.

The water-intake capacity (Table II) increased after the interfacial polymerization of PSf with β-CD-PPI and trimesoyl chloride. This was also ascribed to the improved hydrophilicity as well as the extent of crosslinking during polymerization.

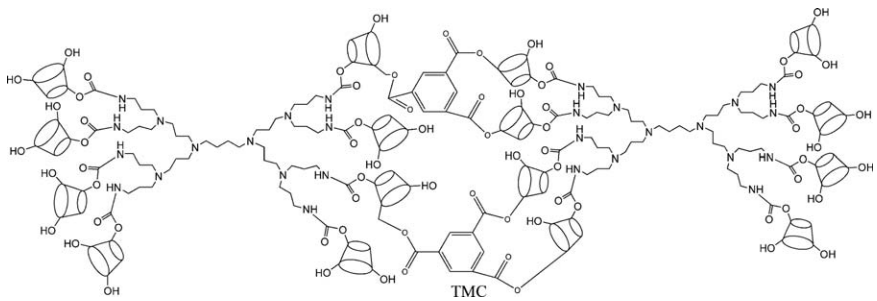


**Scheme 4.** Interfacial polymerization of trimesoyl chloride and the β-CD-PPI conjugate.

Applied Polymer SCIENCE

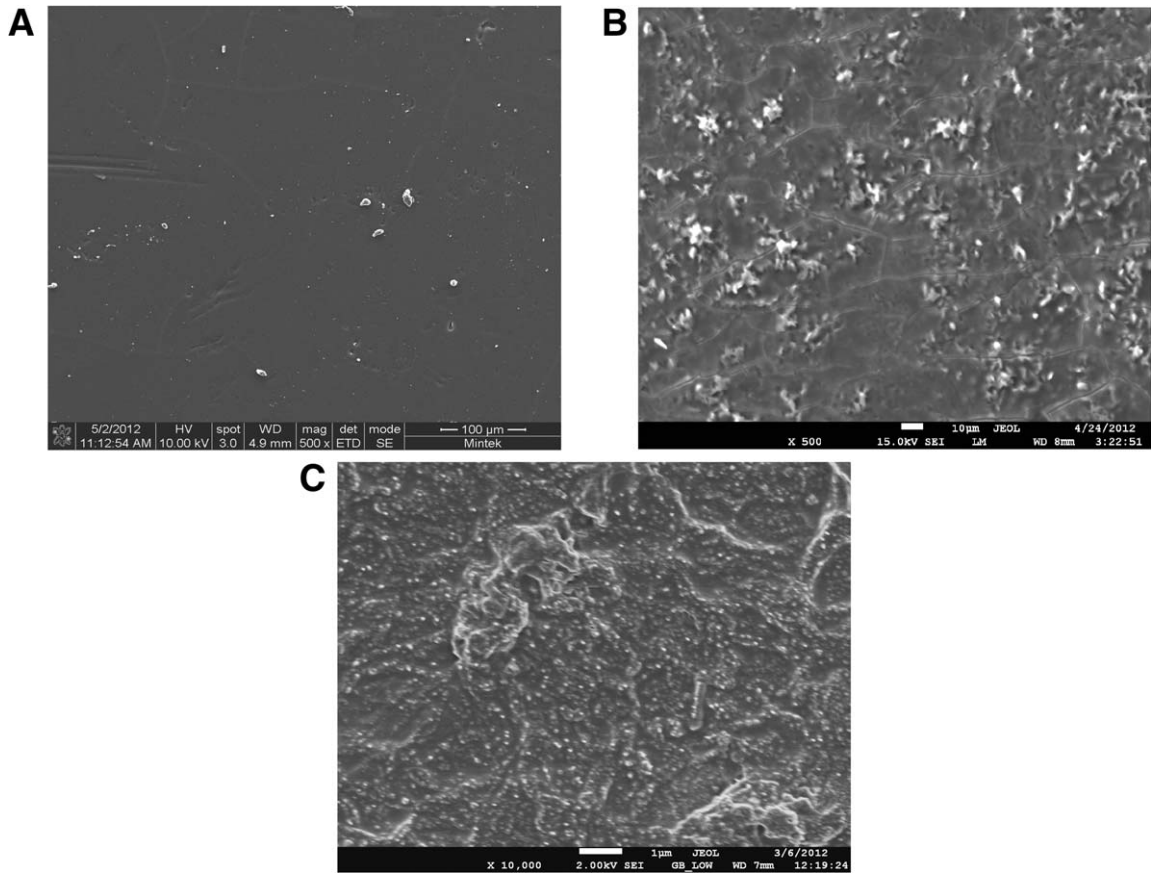


**Figure 5.** SEM images of (A) PSf supporting membrane (×500) (B) β-CD-PPI-PSf membrane (×500), (C) β-CD-PPI-PSf membrane (×10,000).

Generally, when a thin-film composite layer of a modified membrane is not completely crosslinked (as indicated by free OH groups in Figure 4), the structure of the membrane layer tends to be less rigid.[33] This therefore enhances water uptake of the membrane. The adsorptive properties of the membrane can also be improved if the structure is loosely packed since this gives room for the β-CD-PPI to become heavily swollen thus increasing water content.[33]

Figure 7 shows the effect of different pressures on the pure water flux. Generally the flux increased with increasing operating pressure up to 20 bar. The pure water permeability was measured using four different applied pressures and a good linear relationship between the water permeability and applied pressure was observed ($R^2 \approx 0.96$).[33] The commercial PSf membrane had the highest water permeability of 10.09 L $m^{-2}$ $h^{-1}$ $bar^{-1}$ as compared to β-CD-G3-PPI-PSf (2.68 L $m^{-2}$ $h^{-1}$ $bar^{-1}$) and β-CD-G4-PPI-PSf (4.61 L $m^{-2}$ $h^{-1}$ $bar^{-1}$). This low water permeability (Figure 7) and permeate flux [Figure 8(A)] of the modified membranes could be due to the modification and cross linking increasing the path length across the membrane, tightening the effective pore size and partial blocking of the pores. This results in reduced permeability in both clean and fouled water. The decrease in water flux at high polymer loading has been previously observed by Wei et al.[33] and Kim and Deng[24] for PSf-hyperbranched polyether (HPE) membranes and thin-film nanocomposites with hydrophilized ordered mesoporous carbons (H-OMCs). Kim and Deng[24] reported a decrease in the water flux for H-OMCs membranes ($1.45 \times 10^{-1}$ L $m^{-2}$ $psi^{-1}$) at high polymer loading (10%) due to agglomeration of the H-OMCs at very high concentration of the polymer.[17] On the other hand, Wei et al.[33] observed decreased water flux with an increase in HPE loading. At low HPE dosage (1.14 g) a flux of 80 L $m^{-2}$ $h^{-1}$ was recorded and as the dosage of HPE was increased to 5 g the flux decreased to 20 L $m^{-2}$ $h^{-1}$.

Figure 8(B) also shows humic acid rejection as a function of time. β-CD-G3-PPI-PSf and β-CD-G4-PPI-PSf were found to exhibit the highest rejection of ~72% while PSf attained only 57% removal of humic acid. It can be noted that the pore size of the PSf (4.8 nm) is larger than the diameter of the humic acid molecule (2.1 nm) thus it was expected that this membrane would have the lowest rejection (~57%). The larger pore size provided easy passage of humic acid thus it could easily pass through the membrane. Fu et al.[35] reported that low rejections of membranes indicate that the pore sizes of the membrane are much larger than the humic acid molecule size.[35] The presence of the β-CD-PPI resulted in partial blocking of pores which resulted in the increase in the rejection of the humic acid. Similar studies where membranes have been used in the rejection of humic acid are shown in Table III. The β-CD-PPI-PSf

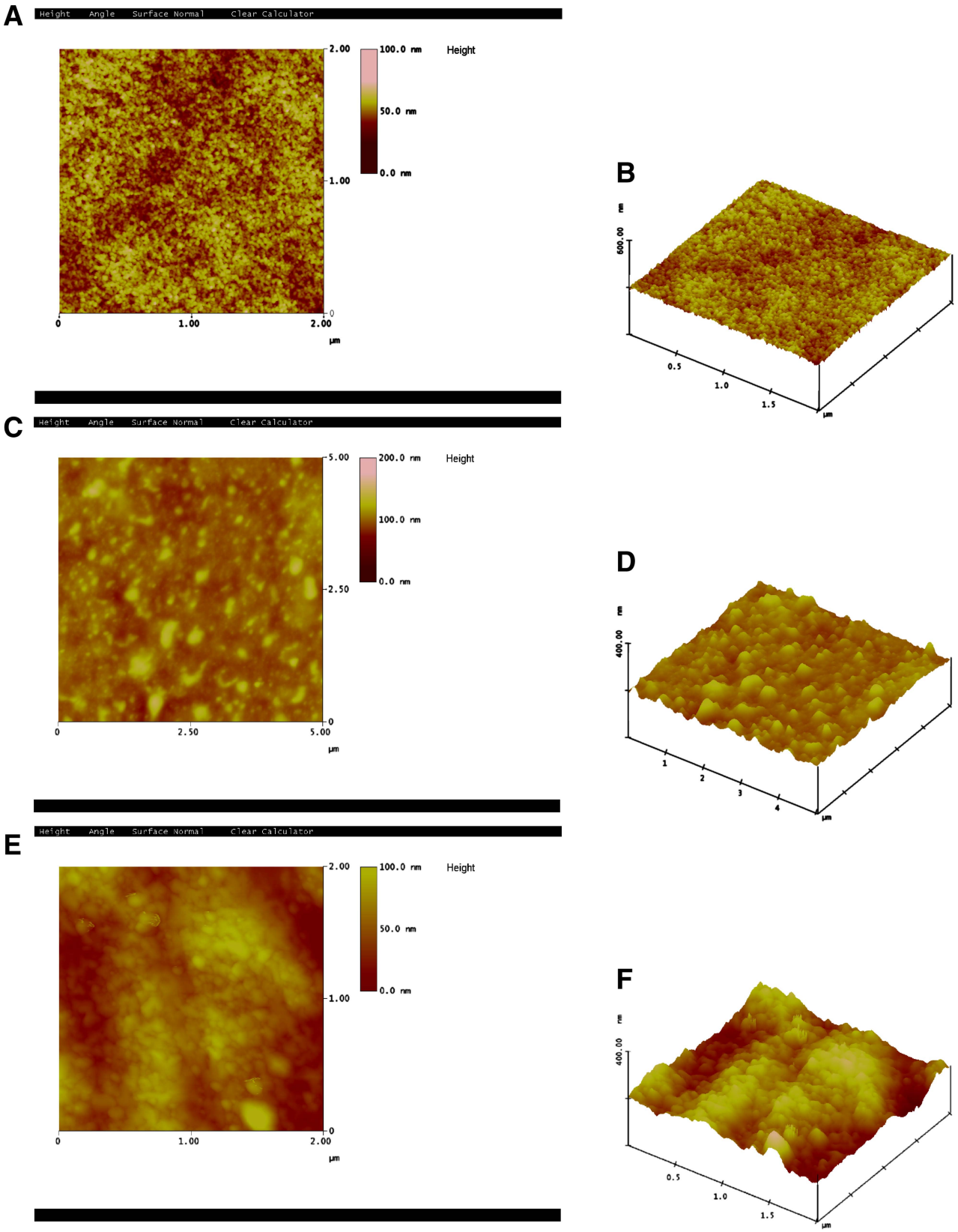


**Figure 6.** A–F: AFM surface images of the membranes: PSf 2D (A), PSf 3D (B), β-CD-G3-PSf 2D (C), β-CD-G3-PSf 3D (D), β-CD-G4-PSf 2D (E), β-CD-G4-PSf 3D (F). [Color figure can be viewed in the online issue, which is available at wileyonlinelibrary.com.]

**Table II.** Water Intake Capacity, Contact Angle, Porosity, Grafting Yield, and Pure Water Flux for PSf and β-CD-PPI-PSf Membranes

| Membranes | Water intake capacity (%)[a] | Contact angle (°) | Porosity (%)[b] | Grafting yield (%)[c] | Pure water permeability (L $m^{-2}$ $h^{-1}$ $bar^{-1}$) |
|---|---|---|---|---|---|
| Commercial PSf | 17 | 76 | 15 | - | 10.09 |
| β-CD-G3-PPI-PSf | 29 | 36 | 23 | 31 | 2.68 |
| β-CD-G4-PPI-PSf | 47 | 41 | 42 | 20 | 4.61 |

[a] Calculated using eq. (2).
[b] Calculated using eq. (3).
[c] Calculated using eq. (1).

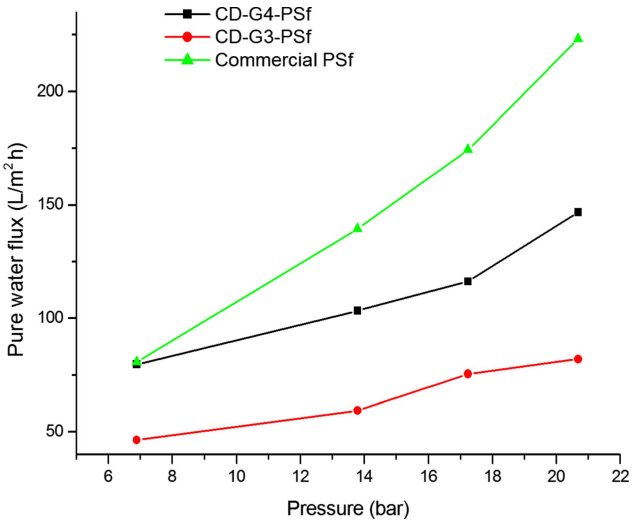


**Figure 7.** The relationship between pure water flux and pressure. [Color figure can be viewed in the online issue, which is available at wileyonlinelibrary.com.]

membranes prepared in this work were found to have comparable humic acid rejection and permeate flux results with those reported in the literature.

***FT-IR analyses of used membranes.*** FT-IR has previously been used by various researchers to assess the fouling of membranes.[38] Comparison of the FT-IR spectrum of fouled PSf membranes and that of the clean membrane shows formation of new bands [Figure 9(A)]. A broad band at 3304 $cm^{-1}$ and a small shoulder observed at 1638 $cm^{-1}$ were ascribed to O—H and aromatic groups (emanating from the humic acid molecule), respectively. This provided evidence that there is interaction of humic acid and the surface of the membrane and this was also confirmed by an increase in contact angle from 76° before humic acid adsorption to 81° after humic acid adsorption. These results are in agreement with those of Yuan and Zydney[39], who found that humic acid deposits on the upper surface of the membrane have a much greater effect on the contact angle. The reduction of the peak at 1702 $cm^{-1}$ (NH—C═O) for the used membranes (β-CD-G3-PPI-PSf and β-CD-G4-PPI-PSf) may also be used as an indication of humic acid deposition on the membrane. The humic acid is capable of

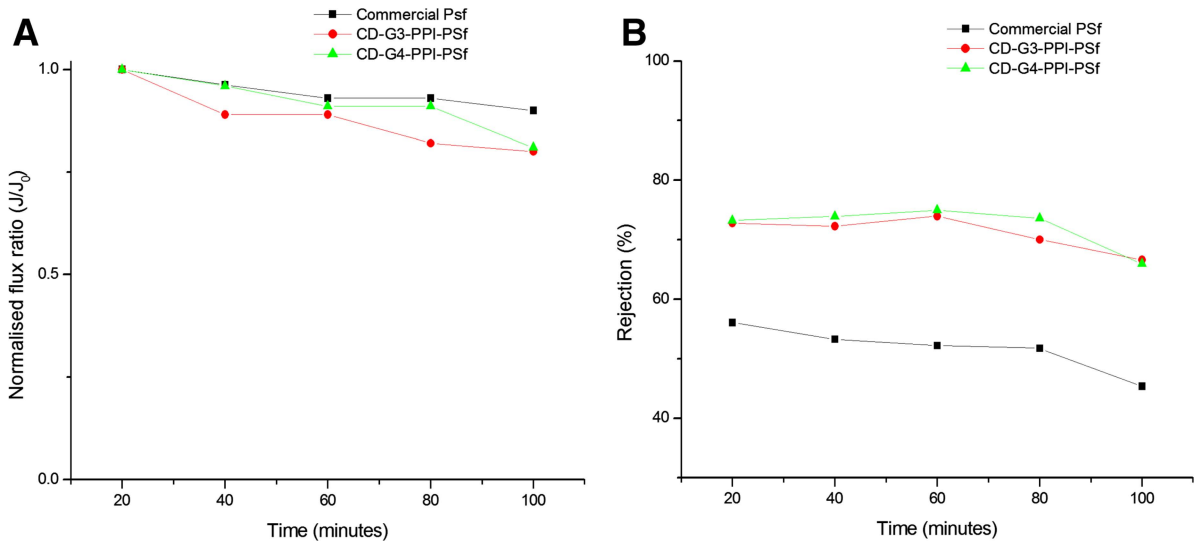


**Figure 8.** Normalized flux ($J/J_0$) for PSf and β-CD-PPI-PSf membranes (A) and rejection of humic acid as a function of time (B). [Color figure can be viewed in the online issue, which is available at wileyonlinelibrary.com.]

**Table III.** Previous Work on Membranes for Humic Acid Rejection

| Membrane | Permeate flux (L $m^{-2}$ $h^{-1}$) | Rejection (%) | Reference |
|---|---|---|---|
| PSf/titanium dioxide ultrafiltration membrane | 0.77-0.8[a] | ~70-90% | 35 |
| Polyphenylsulfone/polyetherimide blend ultrafiltration membranes (E10) | 50 | 79% | 36 |
| Polyacrilonitrile/polyvinylchloride (XM 300) | 70 | ~60% | 37 |
| Uv-grafted polyethersulfone membrane | 0.9[a] | ~98% | 37 |
| $\beta$-CD-G3-PPI-PSf | 45 | ~72% | This work |
| $\beta$-CD-G4-PPI-PSf | 35 | ~72% | This work |

[a] Permeate flux reported as ratio (no units).

blocking the membrane functional group thereby reducing its intensity [Figure 9(C,D)]. Mozia et al.[38] reported that the strong reduction of a band at 1770 $cm^{-1}$ on their cellulose acetate membranes was as a result of humic acid deposits. The presence of humic acid (in our case) was also revealed by the appearance of a new peak at 1640 $cm^{-1}$ for both membranes. After humic acid adsorption by the modified membranes, a slight change in the contact angles was observed. The contact angle for $\beta$-CD-G3-PPI-PSf membrane increased slightly from 36° to 38° while that of $\beta$-CD-G4-PPI-PSf decreased from 41° to 38°. These

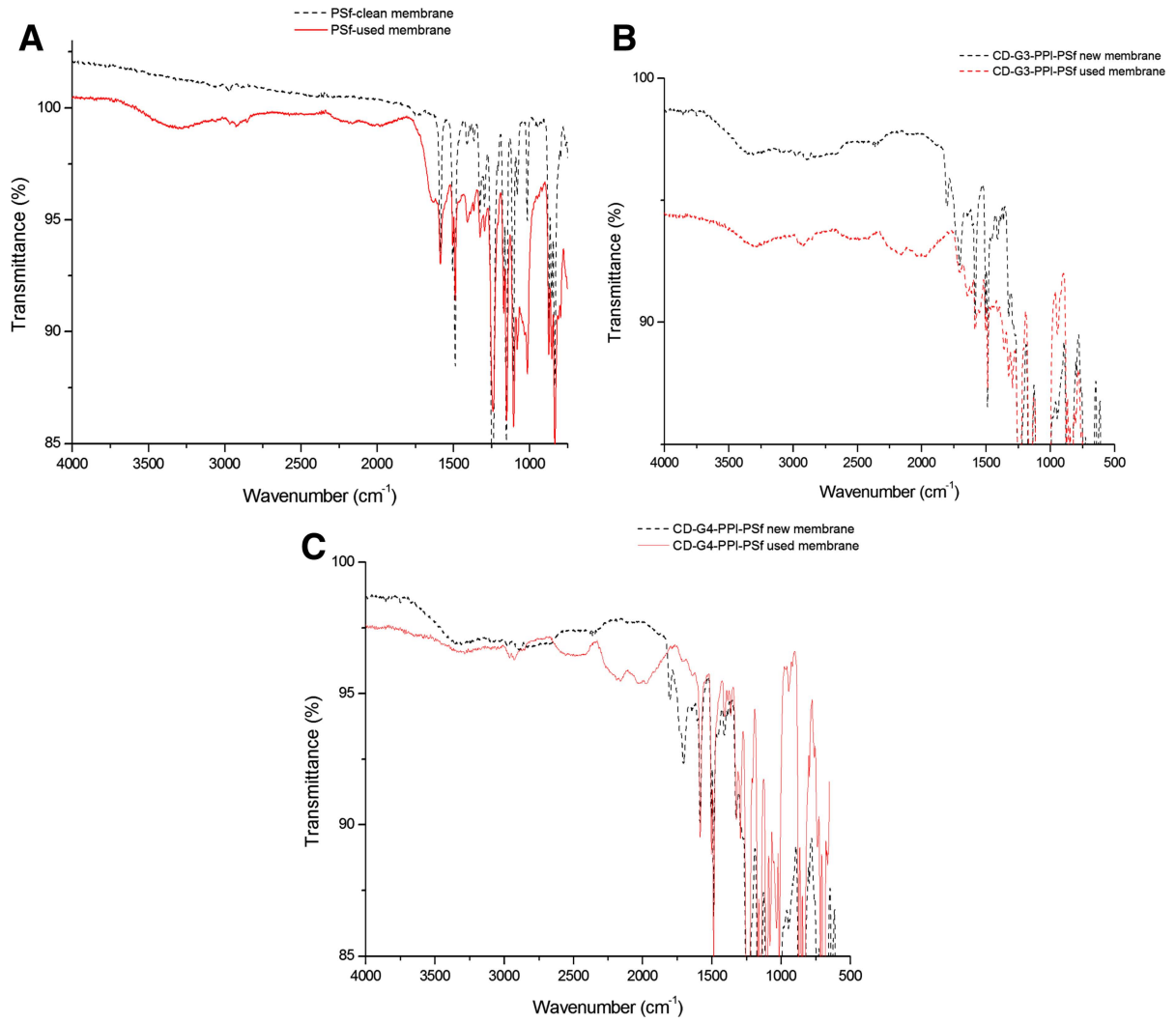


**Figure 9.** FTIR-ATR of clean and used membranes for (A) commercial PSf; (B) $\beta$-CD-G3-PPI-PSf: (C) $\beta$-CD-G4-PPI-PSf. [Color figure can be viewed in the online issue, which is available at wileyonlinelibrary.com.]

observations further confirm that membranes with a higher degree of hydrophilicity (36°–41°) are less susceptible to fouling.[36]

## CONCLUSION

New types of nanostructured composite membranes were developed containing cyclodextrin-poly (propyleneimine) dendrimer. The study revealed that the modification of a polysulfone membrane with $\beta$-CD-PPI nanostructure improves the hydrophilicity of the membrane and separation performance toward humic acid as compared to bare PSf. The presence of $\beta$-cyclodextrin poly (propyleneimine) played an important role in creating water channels for water to pass through and also by restricting humic acid molecules by size exclusion mechanism. However, work is still underway to investigate the stability of the cyclodextrin-dendrimer surface layer in terms of leaching into the permeate as well as recyclability of the membranes.

## ACKNOWLEDGMENTS

The author (SM) is grateful to the University of Johannesburg New Generation Scholars (NGS) Programme for financial support.

## REFERENCES

1. Shao, J.; Hou, J.; Song, H. *Water Res.* **2010**, *45*, 473.
2. Wang, S.; Ma, Q.; Zhu, Z. H. *Fuel Process. Technol.* **2009**, *90*, 375.
3. Schafer, A. I. Natural Organics Removal Using Membranes, Ph.D. Thesis, University of New South Wales, Sydney, Australia, October **1999**.
4. Leiknes, T. *J. Environ. Sci.* **2009**, *21*, 8.
5. Adams, F. V.; Nxumalo, E. N.; Krause, R. W. M.; Hoek, E. M. V.; Mamba, B. B. *J. Membr. Sci.* **2012**, *405/406*, 291.
6. Mbuli, M. B.; Dlamini, D. S.; Nxumalo, E. N.; Krause, R. W.; Pillay, V. L.; Oren, Y.; Linder, C.; Mamba, B. B. *J. Appl. Polym. Sci.* **2013**, *129*, 549.
7. Li, N.; Wei, X.; Mei, Z.; Xiong, X.; Chen, S.; Ye, M.; Ding, S. *Carbohydr. Res.* **2011**, *346*, 1721.
8. Oliveira, J. M.; Salgado, A. J.; Sousa, N.; Mano, J. F.; Reis, R. L. *Prog. Polym. Sci.* **2011**, *35*, 1163.
9. Mamba, B. B.; Krause, R. W.; Malefetse, T. J.; Gericke, G.; Sithole, S. P. *J. Water Supply Res. Technol. AQUA.* **2009**, *58*.44, 299.
10. Mamba, B. B.; Krause, R. W.; Malefetse, T. J.; Mhlanga, S. D.; Sithole, S. P.; Salipira, K. L.; Nxumalo, E. N. *Water SA.* **2007**, *33*, 223.
11. Lukhele, L. P.; Krause, R. W. M.; Nhlabatsi, Z. P.; Mamba, B. B.; Momba, M. N. B. *Desalination Water Treat.* **2011**, *27*, 299.
12. Mamba, B. B.; Krause, R. W.; Malefetse, T. J.; Sithole, S. P.; Nkambule, T. N. *Water SA.* **2009**, *35*, 117.
13. Seman, M. N. A.; Khayet, M.; Hilal, N. *Desalination* **2012**, *287*, 19.
14. Arima, H.; Motoyama, K.; Higashi, T. *Pharmaceutics* **2012**, *4*, 130.
15. Chen, Y.; Zhou, L.; Pang, Y.; Huang, W.; Qiu, F.; Jiang, X.; Zhu, X.; Yan, D.; Chen, Q. *Bioconjugate Chem.* **2011**, *22*, 1162.
16. Sarkar, A.; Carver, P. I.; Zhang, T.; Merrington, A.; Bruza, K. J.; Rousseau, J. L.; Keinath, S. E.; Dvornic, P. R. *J. Membr. Sci.* **2010**, *349*, 421.
17. Shao, L.; Chung, T.-S.; Hong, S.; Pallathadka, K. *J. Membr. Sci.* **2004**, *238*, 153.
18. Taniguchi, I.; Duan, S.; Kazama, S.; Fujioka, Y. *J. Membr. Sci.* **2008**, *322*, 277.
19. Kai, T.; Kouketsu, T.; Duan, S.; Kazama, S.; Yamada, K. *Sep. Purif. Technol.* **2008**, *63*, 524.
20. Duan, S.; Taniguchi, I.; Kai, T.; Kazama, S. *J. Membr. Sci.* **2012**, *423/424*, 107.
21. Choi, S. H.; Chung, J. W.; Priestley, R. D.; Kwak, S.-Y. *J. Membr. Sci.* **2012**, *409/410*, 75.
22. Kang, G.-D.; Cao, Y.-M. *Water Res.* **2011**, *46*, 584.
23. Tang, B.; Huo, Z.; Wu, P. *J. Membr. Sci.* **2008**, *320*, 198.
24. Kim, E.-S.; Deng, B. *J. Membr. Sci.* **2011**, *375*, 46.
25. Singh, K.; Ingole, P. G.; Bhrambhatt, H.; Bhattachayra, A.; Bajaj, H. C. *Sep. Purif. Technol.* **2011**, *78*, 138.
26. Zhang, W.; Cheng, Z.; Song, X.; Si, J.; Tang, G. *Technol. Cancer Res. T.* **2008**, *7*, 103.
27. Madaeni, S. S.; Zinadini, S.; Vatanpour, V. *J. Membr. Sci.* **2011**, *380*, 155.
28. Jin, X. U. E.; Huang, X.; Hoek, E. M. V. *Environ. Sci. Technol.* **2009**, *43*, 3580.
29. Ghosh, A. K.; Hoek, E. M. V. *J. Membr. Sci.* **2009**, *336*, 140.
30. Geens, J.; Boussu, K.; Vandecasteele, C.; Van der Bruggen, B. *J. Membr. Sci.* **2006**, *281*, 139.
31. He, D. *Studies of PPI Dendrimers—Structures, Properties, and Potential Applications*, MS Thesis, The Graduate College of Marshall University, Huntington, WV, August **2002**.
32. Chiang, Y.-C.; Hsub, Y.-Z.; Ruaan, R.-C.; Chuang, C.-J.; Tung, K.-L. *J. Membr. Sci.* **2009**, *326*, 19.
33. Wei, X.-Z.; Zhu, L.-P.; Deng, H.-Y.; Xu, Y.-Y.; Zhu, B.-K.; Huang, Z.-M. *J. Membr. Sci.* **2008**, *323*, 278.
34. Kang, G.; Liu, M.; Lin, B.; Cao, Y.; Yuan, Q. *Polym. Commun.* **2007**, *48*, 1165.
35. Fu, X.; Maruyama, T.; Sotani, T.; Matsuyama, H. *J. Membr. Sci.* **2008**, *320*, 483.
36. Hamid, N. A. A.; Ismail, A. F.; Matsuura, T.; Zularisam, A. W.; Lau, W. J.; Yuliwati, E.; Abdullah, M. S. *Desalination* **2011**, *273*, 85.
37. Hwang, L.-L.; Tseng, H.-H.; Chen, J.-C. *J. Membr. Sci.* **2011**, *384*, 72.
38. Mozia, S.; Tomaszewska, M.; Morawski, A. W. *Water Res.* **2005**, *39*, 501.
39. Yuan, W.; Zydney, A. L. *Environ. Sci. Technol.* **2000**, *34*, 5043.